Electric Propulsion R&D at Osaka Institute of Technology

IEPC-2017-83

Presented at the 35th International Electric Propulsion Conference
Georgia Institute of Technology • Atlanta, Georgia • USA
October 8 – 12, 2017

Ryota Fujita[1], Hirokazu Tahara[2], and Kyoko Takada[3]
Osaka Institute of Technology, 5-16-1, Omiya, Asahi-Ku, Osaka, 535-8585, Japan

Abstract: At Osaka Institute of Technology, four kinds of electric propulsions and micro/nano satellites have been investigated and developed. A radiation-cooled MPD thruster with simple structure by using permanent magnets has been developed for manned Mars exploration. A steady-state arcjet thrusters have been developed for satellite attitude control and orbital transfer. A pulsed plasma thruster by using solid propellant for micro/nano satellite has been developed. Three types of Hall thruster have been investigated. The 2nd PROITERES was determined to be launched by H-IIA rocket of JAXA on July in 2008. In the present paper, we introduce all activities of electric propulsions R&D at OIT.

I.Introduction

At Osaka Institute of Technology, lots kinds of electric thrusters have been investigated and developed as shown in Fig.1; R&D of micro/nano satellites with their thrusters are under way. In the present paper, we introduce all activities of electric propulsion R&D at OIT.

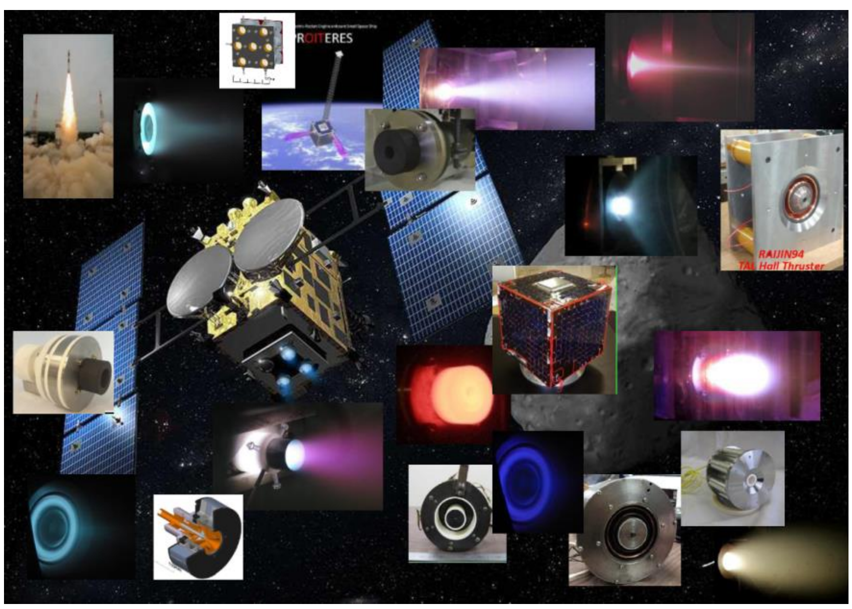

Figure 1. Overview of electric propulsion R&D at Osaka Institute of Technology and JAXA HAYABUSA2.

[1] Graduate Student, Major in Mechanical Engineering, and hirokazu.tahara@oit.ac.jp.
[2] Professor, Department of Mechanical Engineering, and hirokazu.tahara@oit.ac.jp.
[3] Associate Professor, Department of Intellectual Property, and kyoko.takada@oit.ac.jp.

II.MPD thruster

Steady-state MPD thrusters have been investigated by experiment and analysis at Osaka Institute of Technology. In this study, a practical MPD (Magneto-Plasma-Dynamic) thruster system was developed for In-space missions as one of the In-Space Propulsion project in collaboration with the Japan Aerospace eXploration Agency (JAXA).

In experiment, in order to make the system easier, the MPD thruster we developed is equipped with permanent magnets. In this research, shapes of a magnetic field were changed to cusp field. Therefore, the decrease in discharge voltage was anticipated and aimed at improvement of the thrust efficiency. And an electrode was changed to straight-divergent nozzle. Therefore, the drop of the speed loss of the propellant and the improvement of the thrust efficiency were anticipated. The final targets are to achieve thrust performances, a thrust of 0.5-2.0 N, a specific impulse of 1,000-3,000 s and a thrust efficiency of 40% [1].

In analysis, a fully radiation-cooled (FRC) MPD thruster was designed for the purpose of practical use. As aims of this research, temperature of permanent magnet is made lower than irreversible demagnetization temperature. And, structure suitable for complete radiation-cooled MPD thruster is made decide from analysis results [2].

A. Experimental devices

Figure 2 shows the 3D model the MPD thruster with divergent field and the MPD thruster with cusp field used for this study [3-5], respectively. The thruster was operated with an input power of 5-10 kW.

The MPD thruster has a magnetic circuit which is formed by iron plates sandwiched SmCo magnets around the anode for application of axial magnetic field. Figure 3 shows the MPD thruster with divergent field lines and cusp field lines calculated by an analytic software (Tricomp), respectively. As shown in Fig. 3 (a), they were parallel to the central axis in the constrictor. The maximum strength of magnetic field was approximately 0.157 T near the constrictor measured with a Gauss meter. Also, because the magnets can be equipped individually, the strength of magnetic field can be changed. As shows in Fig. 3 (b), cusp shape is formed at the position of central iron plate made in SS400 put to the permanent magnets. Therefore, the performance acquisition by the change is possible at a cusp position.

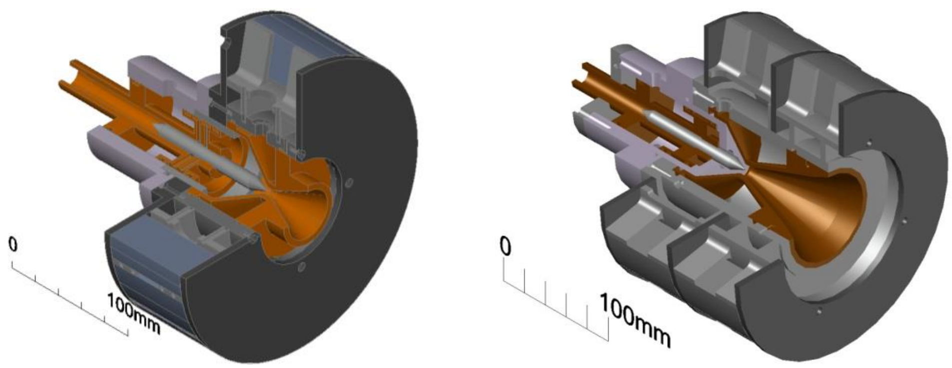

(a) The MPD thruster with divergent field **(b) The MPD thruster with cusp field**

Figure 2. 3D models of the MPD thruster.

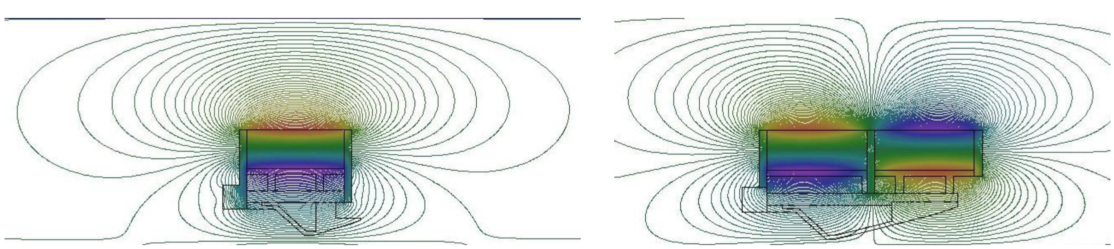

(a) The divergent field **(b) The cusp field**

Figure 3. Magnetic field of the MPD thruster.

B. Experiment of MPD thruster with divergent magnetic field

Table 1 shows experimental conditions. Anodes with diameters of 2 mm and 10 mm were used for this experiment. As the propellant, ammonium was used.

Table 1. Experimental conditions.	
Propellant	NH3
Constrictor Diameter, mm	2, 10
Mass Flow Rate, mg/s	5, 60, 150
Magnetic Flux Density, T	0.157
Discharge Current, A	70-150

Figure 4 shows operations using the anodes which have diameters of 2 and 10 mm, respectively. In the case of operation using the anode with a diameter of 10 mm, the plasma plume was converged on the center axis. However, the convergence of plasma plume was not observed using the anode with a diameter of 2 mm. It was considered that electrothermal acceleration was main acceleration with the anode having a diameter of 2 mm because the pressure in the discharge room was very high.

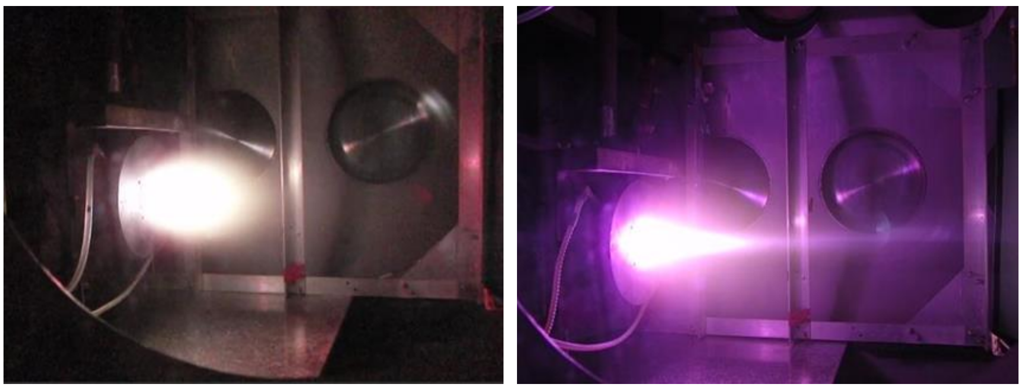

(a) Diameter of 2 mm **(b) Diameter of 10 mm**

Figure 4. Plasma plumes of NH_3, 150 mg/s.

The performance characteristics are shown in Fig. 5. As shown in Fig. 5 (a), the thrust increased as the discharge current increased. The thrust efficiency in large flow rate was higher than that in small flow rate (see in Fig. 5 (b)). In the case of large flow rate, it was confirmed the thrust and discharge voltage was high. The thrust efficiency was known to be proportional to the square of the thrust value and to be inversely proportional to discharge voltage. Therefore, the thrust efficiency was higher in large flow rate. Typical performance with NH^3, a thrust of 477.4 mN, a specific impulse of 811.4 s and a thrust efficiency of 19.0%, were obtained at 0.157 T.

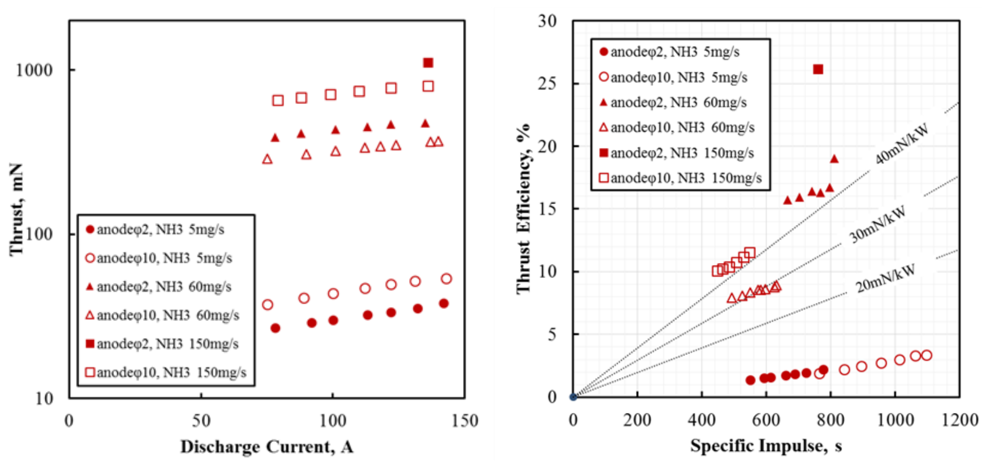

(a) Thrust vs. discharge current **(b) Thrust efficiency vs. specific impulse**

Figure 5. The performance characteristics.

C. Experiment of MPD thruster with cusp field

The MPD thruster with cusp field was developed, applied experiment, and acquired performance. And, the performance of MPD thruster with cusp field and MPD thruster with divergent field was compared. Experiments were conducted at three places of -5, 0, +5 mm and performance characteristics were acquired. Figure 6 represents the schematic view of the cusp position. Figure 7 shows the experimental results.

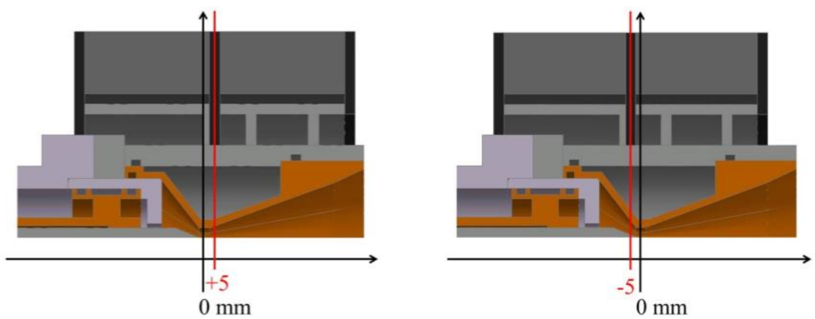

(a) +5mm **(b) -5mm**

Figure 6. Schematic view of the cusp position.

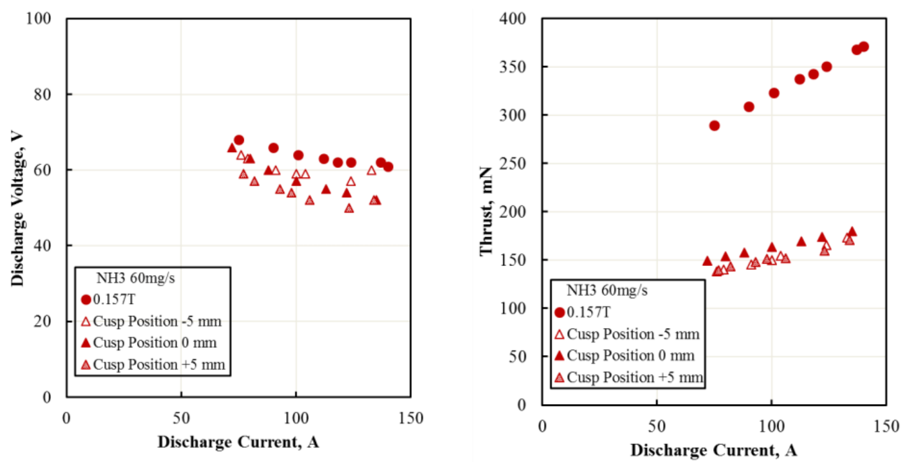

(a) Discharge voltage vs. discharge current **(b) Thrust vs. discharge current**

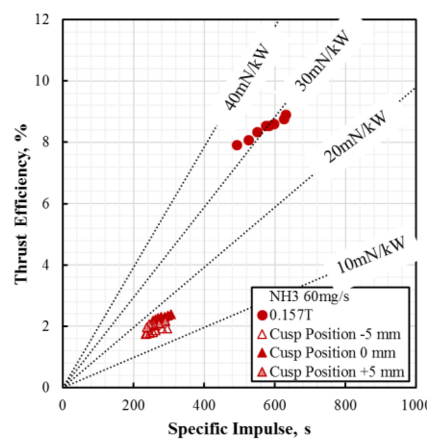

(c) Thrust efficiency vs. specific impulse

Figure 7. Experimental results.

As shown in Fig. 7 (a), the discharge voltage decreased with increased the discharge current. In addition, it was confirmed that the discharge voltage decreased by applying the cusp field. Figure 7 (b) shows thrust vs. discharge current. As shown in Fig. 7 (b), compared to the MPD thruster with cusp field, the MPD thruster with divergent field increased. It is considered that the Lorentz force due to the applied cusp field became an obstacle to acceleration. Finally, Fig. 7 (c) shows thrust efficiency vs. specific impulse. By using the cusp field, the discharge voltage decreased, but the thrust became small. Therefore, the MPD thruster with divergent field resulted in higher thrust efficiency. In the future, it is necessary to change the cusp position and find the condition that the thrust is difficult to decrease.

D. Thermal analysis of fully radiation-cooled MPD thruster

A fully radiation-cooled (FRC) MPD thruster was designed so that magnetic circuit of water-cooled MPD thruster can be reused. Figure 8 (a) show 3D model of the previous structure of FRC-MPD thruster (structure 1). Parts of FRC-MPD thruster are anticipated increasing temperature, because of without water-cooled. Therefore, most thruster parts were constitute refractory material, (pure tungsten, TZM). Characteristics of structure 1 is seen in Fig. 8 (b). First, heat to conduct to radial direction is controlled with insulator. Second, metal parts which was located inside of insulator make to conduct heat to axial direction. And, heat is conducted to the backward of thruster. Finally, heat is discharged in space through radiation plate.

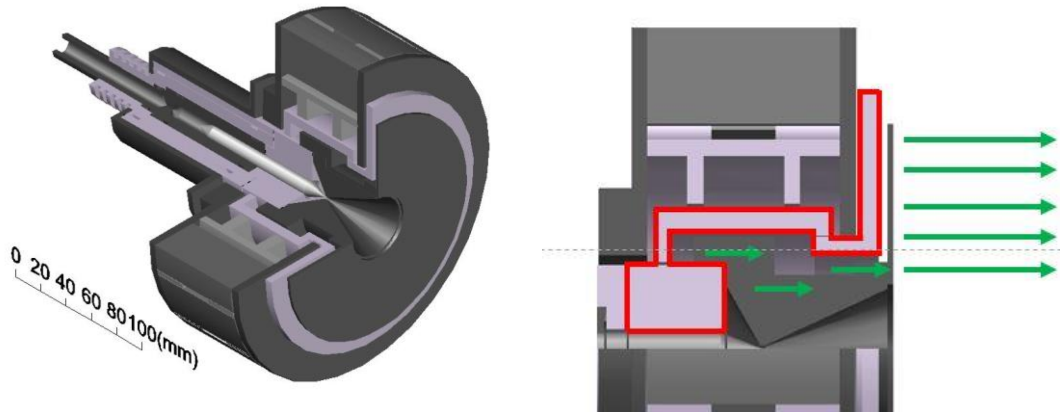

(a) 3D model **(b) Characteristics of structure 1**

Figure 8. FRC-MPD thruster.

In this research, thermal analysis was carried out with Thermal Desktop (C&R Technologies, Inc.). Structure of FRC-MPD thruster was examined that could be decreasing steady-state temperature distribution of SmCo magnet. Permanent magnet was have irreversible demagnetization temperature, it were mentioned above. Therefore, optimum structure of FRC-MPD thruster was defined a structure as temperature of permanent magnet lower than irreversible demagnetization temperature of SmCo (620 K).

FRC-MPD thrusters changing structure were developed based on a previous structure of FRC-MPD thruster (structure 1). They were developed 3 type. And, they were called structures 2, 3, 4, respectively. Fig. 9 shows analysis models of structures 1 - 4. Structure 1 was a previous structure of FRC-MPD thruster. Characteristics of structure 2 was located an insulator with the thickness instead of metal parts of structure 1. Therefore, heat to conduct to radial direction was going to restrain than structure 1. Characteristics of structure 3 was divided an insulator into three parts. So, not only structure 3 but also a multi-layer insulator FRC-MPD thruster were called. The concept was to restrain to conduct to heat by thermal conduction, and to promote to conduct to heat by heat transfer. Characteristics of structure 4 was changed the material of the center of the three parts to tungsten from ceramic. Therefore, heat to conduct to radial direction was going to restrain by insulation effect with materials, and was promoted heat to conduct to axial direction.

4 types of FRC-MPD thruster were analyzed with analysis conditions. Analysis conditions were calculated from experimental results at 8.0 kW. The analysis time was installed steady-state. Applied heat to the cathode and the anode were 300 W and 4,770 W, respectively. The most suitable structure of the electric discharge room circumference was postulated that lowest structure of steady-state temperature of permanent magnet. In this analysis, the temperature change of permanent magnet was compared by changing structure of the electric discharge room circumference.

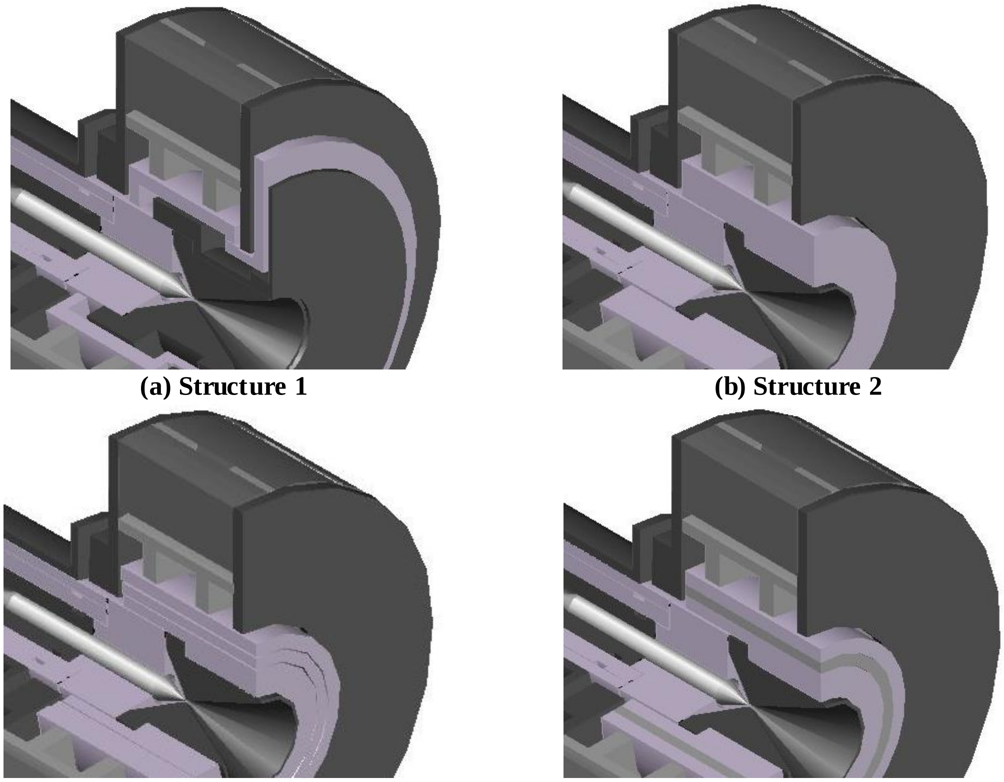

(a) Structure 1 (b) Structure 2

(c) Structure 3 (d) Structure 4

Figure 9. Analysis models.

Table 2 shows maximum temperature and minimum temperature of permanent magnet of structures 1 - 4, respectively. As the results, structure 1 was highest temperature of permanent magnet. And, structure 4 was lowest temperature of permanent magnet. The difference of temperature of structures 1 and 4 were 110 K. From these results, characteristics of previous structure was not suitable structure of FRC-MPD thruster. As a cause of temperature rise, it is thought that heat to conduct to radial direction was not able to prevent by lack of thickness of insulator. Thickness of insulator of structure 1 was half of other structure. So, insulation effectiveness was appeared conspicuously by thickness of insulator that compare structure 1 and structure 2. Therefore, it is thought that mounting of insulator with thickness is effective. And, the difference of temperature of structures 1 and 2 were 26 K.

Temperature distribution of structure 3 was lower than structure 2. Also, the difference of temperature of structures 2 and 3 were 80 K. This result was appeared insulation effectiveness by increasing insulator parts. In other words, this insulation effectiveness is thought that mechanism of conduct to heat is difference between heat transfer and thermal conduction. So, the heat transfer conduction (heat transfer) with parts more plural can restrain the heat of the diameter direction than the conduction heat transfer (thermal conduction) with one part.

Temperature distribution of structure 4 was lower than structure 3. Also, the difference of temperature of structures 3 and 4 were 4 K. This insulation effectiveness was the influence of changing the material of the center of the three parts to pure tungsten (W) from ceramic. That is, difference of characteristics of materials produced insulation effectiveness. However, temperature change was low. Also, it is thought the analysis error by mesh shapes.

Finally, structure 4 can be assumed the most suitable structure of FRC-MPD thruster by changing structure.

Table 2. Temperature of permanent magnet.

Structure Number	Minimum Temperature, K	Maximum Temperature, K
1	908.1	1,033
2	877.4	1,007
3	834.8	927.1
4	831.1	923.1

III. Arcjet thruster

Characteristics of arcjet thruster is that the thrust is higher than other electric propulsion and it can use propellants together with chemical propulsion. Arcjet thruster is used to satellite attitude control and an orbit control. Hydrazine is propellant that has been used for arcjet thuruster. However, hydrazine has very high in toxicity, it has many problems in terms of time, safety management and cost. Therefore, currently low-toxicity propellants have been advanced as one of the solutions. We focused on water propellant and HAN series propellant as alow-toxicity propellant. In this research, we development of the water-cooled arcjet thruster and the anode-radiation-cooled arcjet thruster[6-12].

A. Water-cooled arcjet thruster

Figure 10 shows water-cooled arcjet thruster, sectional view of water-cooled arcjet thruster and electrode configuration. This arcjet thruster is water cooling both electrodes. The details of the electrode configuration are shown in Table 3.

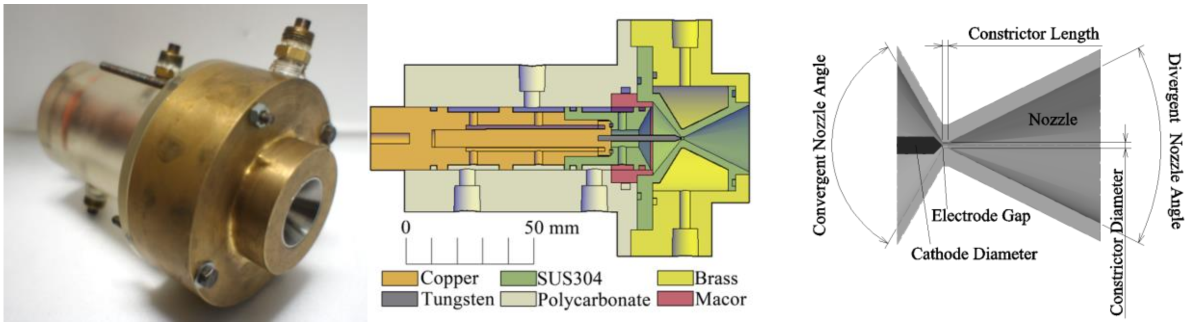

(a) Body **(b) Cross sectional view** **(c) Electrode configuration**

Figure 10. Water-cooled arcjet thruster.

Table 3. Details of electrode configuration (water-cooled).

Cathode Diameter, mm	3.0
Constrictor Length, mm	1.0
Constrictor Diameter, mm	1.0
Divergent Nozzle Angle, deg.	52
Convergent Nozzle Angle, deg.	102
Electrode Gap, mm	0.0

We measured the performance of HAN (SHP163) decomposed gas and compared with that of hydrazine decomposed gas using water-cooled arcjet thruster. Experimental conditions in performance comparison are shown in Table 4.

As shown Fig. 11, thrusts with SHP163 and hydrazine decomposed gases are 105.7 mN and 145.8 mN, respectively, with specific impulses of 214.6 s and 337.8 s at input powers of 1.36 kW and 1.33 kW, and thrust efficiencies are 6.47% and 6.17%, respectively. As a result, thrust performances of SHP163 decomposed gas is lower than that of hydrazine decomposed gas.

Table 4. Experimental conditions.

Propellant	SHP163	Hydrazine
Flow rate, mg/s	40, 50, 60	
Current, A	7.0, 8.0, 9.0, 10.0	
Cathode diameter, mm	2.0	

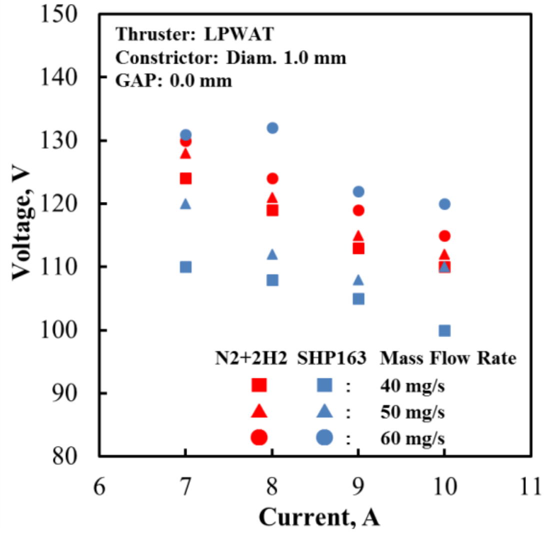

(a) Discharge voltage vs. current

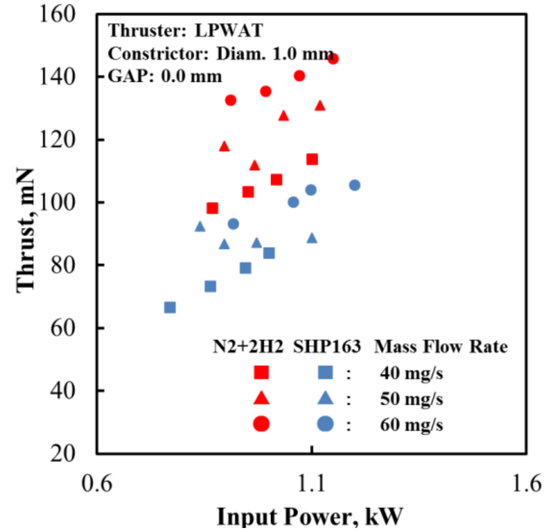

(b) Thrust vs. input power

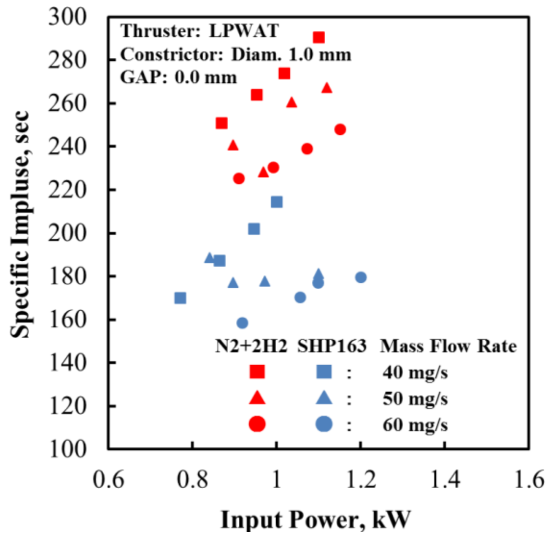

(c) Specific impulse vs. input power

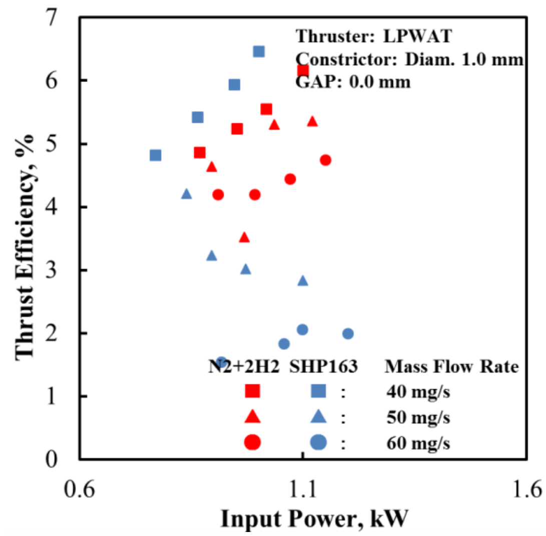

(d) Thrust efficiency vs. input power

Figure 11. Performance comparison of SHP163 and hydrazine decomposed gases.

We performed operation experiments of the water-cooled arcjet thruster using water propellant. In the experiment the gas generator was used, and initial ignition with water propellant and nitrogen was conducted because it is difficult with only water propellant. Just after ignition, we changed operation with only water propellant. Table 5 shows the experiment condition. Although vapor was slightly cooled inside the water-cooled arcjet thruster, we could operate during 10 seconds with only vapor, as shown in Fig. 12, just after ignition with nitrogen mixture

Table 5. Experimental conditions.

Propellant	Water
Flow Rate, mg/s	33.3
Current, A	15
Cathode Diameter, mm	3.0

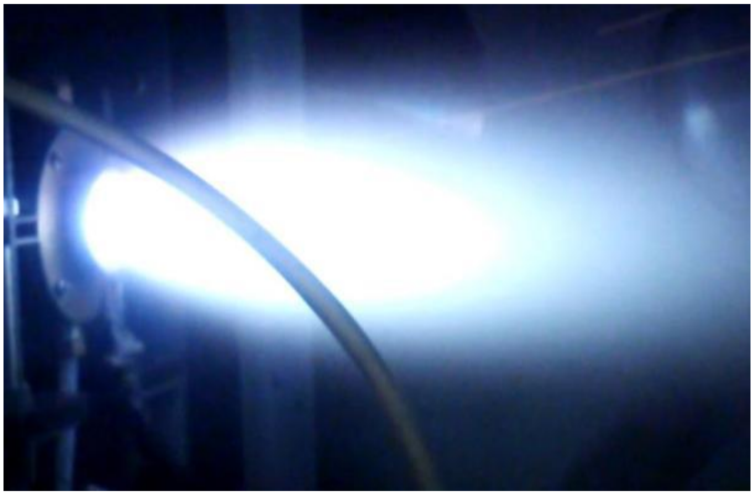

Figure 12. Photo of plasma plume with only water propellant

B. Anode-radiation-cooled arcjet thruster

A anode-radiation-cooled arcjet thruster was design. The FEM analysis to know the temperature distribution was performed on Thermal Desktop (Cullimore and Ring Technologies, Inc). Analysis model of the new anode-radiation-cooled arcjet thruster is shown in Fig. 13 (a) and the schematic view of the heat transfer coefficient definition points is shown in Fig. 13 (b). Also, analysis conditions are shown in Table 6. In this study water cooled condition defines temperature of the water attachment area as 293.15 K. The heat load is applied on the cathode tip was defined 12.0% of total input power. And the heat load to the anode inner surface tip was defined 33.0% of total input power.

The temperature distribution of the anode-radiation-cooled arcjet thruster is shown in Fig. 14. As shown in Fig. 14 (a), all component temperature of the new anode-radiation-cooled arcjet thruster was confirmed lower than the melting point. As shown in Fig. 14 (b), a maximum temperature of approximately 3,286 K was obtained at the cathode tip. The temperature was lower than the melting point of tungsten. As all results of thermal analysis, thermal design of the thruster was acceptable. The development of new anode-radiation-cooled arcjet thruster carried out.

Figure 15 shows anode-radiation-cooled arcjet thruster, sectional view and electrode configuration. In this thruster, the cathode part is water cooling and the anode part is radiation coolimg. The details of the electrode configuration are the same as anode-radiation-cooled arcjet thruster.

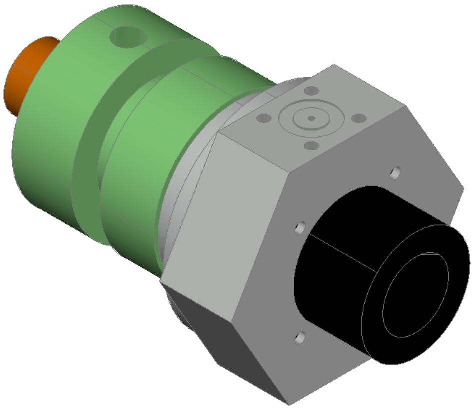

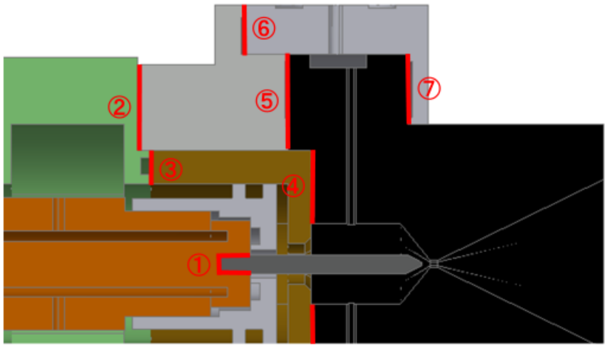

(a) Analysis model **(b) Schematic view**

Figure 13. Anode-radiation-cooled arcjet thruster.

Table 6. Analysis conditions.

Input power, W	Total	1,000
	Cathode	120
	Anode	268
Temperature of water-cooled, K		293.15
Number of mesh	Total	143,358
	Cathode	4,323
	Anode	34,228
Heat transfer coefficient , W/m^{2}K	1	100,000
	2	80
	3	2,082
	4	84,278
	5	345
	6	3,075
	7	4,401

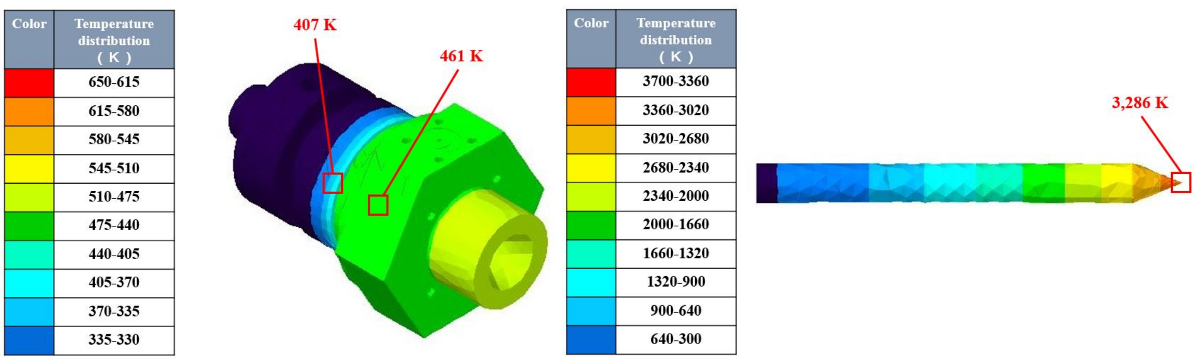

(a) Entire thruster **(b) Cathode**

Figure 14. Analysis results.

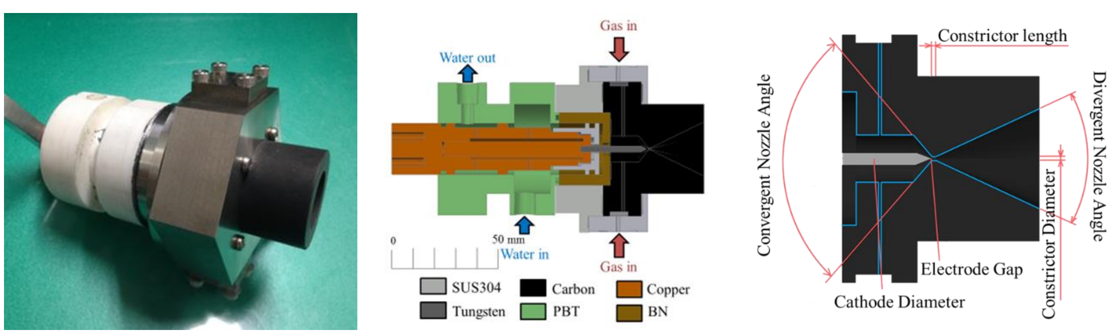

(a) Body **(b) Cross sectional view** **(c) Electrode configuration**

Figure 15. Anode-radiation-cooled arcjet thruster.

We obtained basic performance using the developed thruster and compared it with water-cooled type. Experimental conditions are shown in Table 7.

Table 7. Analysis conditions.

Cooling Type	Anode-radiation-cooled	Water-cooled
Propellant	Nitrogen	
Flow Rate	40,50,60 mg/s	
Current	14,15,16,17 A	

The results of performance are shown in Fig. 16. As a result, when the input power was 0.896 kW and the flow rate was 60 mg/s, the thrust was 179.95 mN, the specific impulse was 306.12 s, and the thrust efficiency was 15.1%. In the case of the water-cooled type, it is considered that the energy necessary for converting the propellant into a plasma was deprived by water cooling as the anode was water-cooled. Therefore, by changing the anode-radiation-cooled, it was possible to eliminate the energy loss that energy is deprived by water cooling.

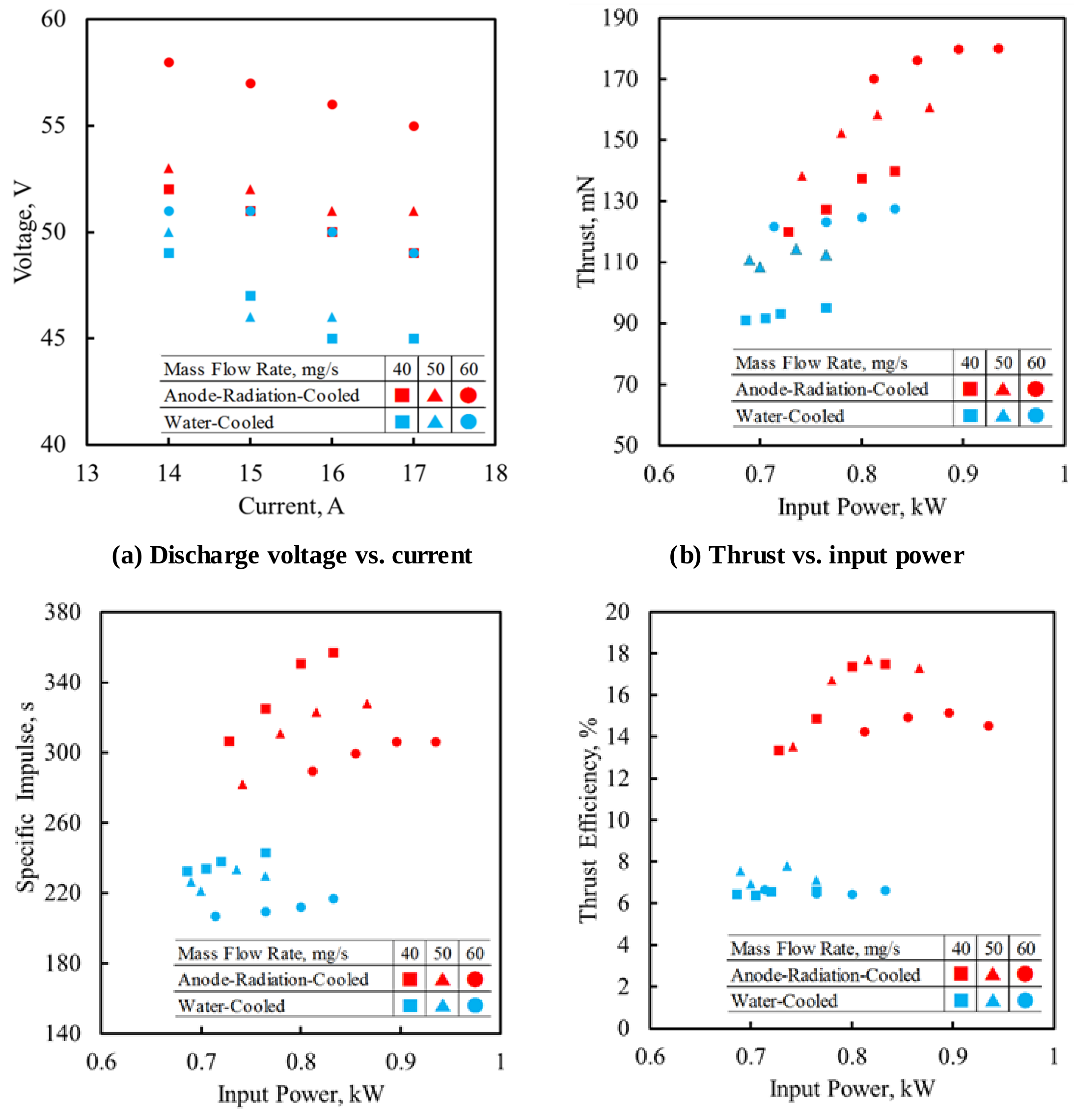

(a) Discharge voltage vs. current

(b) Thrust vs. input power

(c) Specific impulse vs. input power

(d) Thrust efficiency vs. input power

Figure 16. Performance comparison of water-cooled and anode-radiation-cooled arcjet thruster.

C. Conclusion

We carried out the operation confirmation experiment using water-cooled arcjet thruster with water propellant. As a result, we confirmed about 5 Seconds operation time. From this, the possibility of operation with water propellant could be confirmed. We also developed the anode-radiation-cooled arcjet thruster. It is a radiant cooling type for the anode part. The purpose of the development is to improve the performance, aiming for further long-term operation and aiming a preliminary step to actual equipment. In the future, we will carried out performance mesurment experiment for HAN series propellant and conducted operation experiment for water propellant with anode-radiation-cooled arcjet thruster. And, we will develop fully radiant cooled arc jet thruster assuming use of low-toxicity propellant.

IV.PROITERES and PPT

The Project of Osaka Institute of Technology Electric-Rocket-Engine onboard Small Space Ship (PROITERES) was started at Osaka Institute of Technology in 2007. In 1st PROITERES satellite, a nano-satellite with electrothermal-acceleration-type Pulsed Plasma Thrusters (PPTs) was successfully launched by the Indian PSLV C-21 rocket on September 9th, 2012. The main mission is to change an orbital transfer of 1 km as powered-flight by PPT systems and to observe Kansai district in Japan with a high-resolution camera. In the specification of the satellite, the weight is 14.5 kg, the configuration is a 0.29 m cube, and the electric power is 10 W[13,14)].

Now, we are developing the 2nd PROITERES satellite. The R&D of the 2nd PROITERES was started in 2010. The main mission is to achieve longer distance orbital transfer, i.e. changing 50-100 km in altitude on near-earth orbits by longtime operation and high power PPT system. It has been decided that the 50kg class 2nd PROITERES satellite is launched to 613 km in earth altitude by H-IIA rocket at Tanegashima Space Center, Japan Aerospace Exploration Agency (JAXA) on July in 2008. The 2nd PROITERES satellite will be launched by piggyback payloads of GOSAT-2 and Khalifasat. This research aims to develop 30 W class PPT system by numerical calculation and experiment.

In numerical calculation, it is carry out optimization at cavity form for 30 W class PPT, is aims to improves thrust performance[15,16)].

In experiment, the PPT-system of the 2nd satellite has to work with higher electric energies and has to achieve a longer lifetime. As a method to increase the electric energy, a capacitor of the 1st PROITERES was improved from one to thirteen capacitors. Accordingly, the energy in the capacitors could be increased from 2.43 J to 31.59 J. To achieve the longer lifetime, a Multi-Discharge-Room type PPT with seven discharge rooms was developed[17-19)].

A. Numerical calculation

We confirmed the validity of the numerical calculation by compared between experiment and calculation thrust performance results with the 30 W class single cavity type PPT for the 2nd PROITERES. The numerical calculation and experiment conditions is presented in Table 8. Figure 17 shows a schematic of the present calculation.

Table 8. Numerical calculation and experiment conditions.

Cavity length, mm	10/15/20/25/30/35/40/45/50
Cavity diameter, mm	4
Nozzle length, mm	14
Nozzle half angle, deg.	0
Capacitance, μF	19.5
Charging voltage, V	1,800
Input energy, J	31.59
Inductance, μH	0.189
Resistance, mΩ	9.84

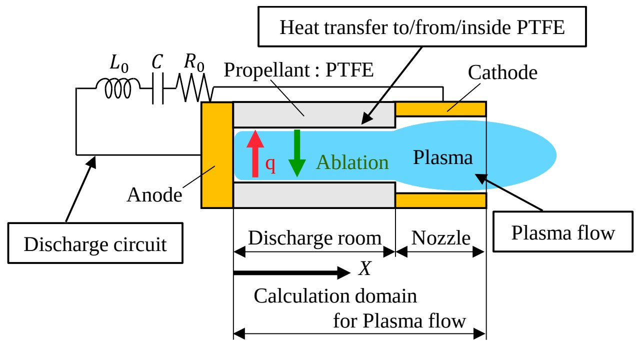

Figure 17. Schematic of the present calculation model.

Figure 18 (a) shows impulse bit and mass loss per shot (mass shot) versus cavity length. Figure 18 (b) shows specific impulse and thrust efficiency versus cavity length. Mass shot is increased as it become longer cavity length because it is increased in cavity volume. Therefore, impulse bit is increased by increment of mass shot. Specific impulse is decreased by smaller impulse bit per mass shot as it become longer cavity length. The cause is considered to decrease energy density and pressure inside cavity. Thrust efficiency is confirmed to maintain certain level. The simulated impulse bit, mass shot, specific impulse, and thrust efficiency is compared experiment results by similar condition, it achieved maximum error at 11%, 14%, 12%, and 25%, respectively, validity of numerical calculation is suggested. The every cavity length confirmed to agree qualitative by comparison between numerical calculation and experiment results.

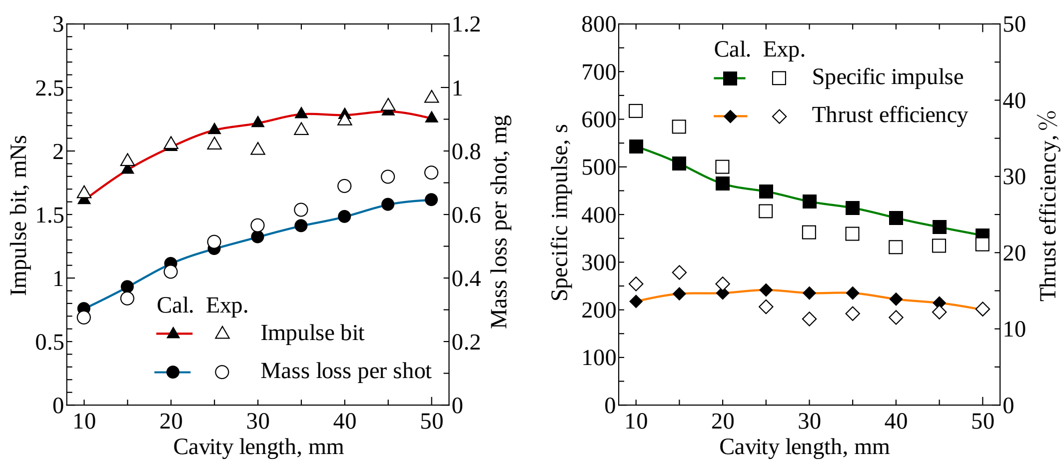

(a) Impulse bit and mass shot vs. cavity length (b) Specific impulse and thrust efficiency vs. cavity length
Figure 18. Comparison of thrust performance between numerical calculation and experiment.

The target of this research is to generate high orbital velocity variation (delta-V) by 2nd PROITERES satellite onboard 30 W class PPT system. In parameter of PPT, generation of high delta-V is most important total impulse. The improving of total impulse will be required high impulse bit and longtime operation. Another electric propulsions using liquid and gas propellant is referring to specific impulse due to a longtime operation, but PPT using solid propellant is referring to extension of cavity diameter in repetitive operation because it finishes operation generates in the charring at cavity wall with equal diameter of cavity and nozzle. In previous research, longtime repetitive operation experimental by extension nozzle diameter carried out, but was not carried out operation. The cause is no inflow inside cavity with generated electron by ignition discharge in too big nozzle diameter. It is difficult to equip nano-satellite with PPT too large nozzle diameter. Therefore, the repetitive operation simulation of 10,000 shots with cavity length between 10 and 50 mm carried out, it simulated changes in the cavity diameter. The conditions of this simulation is same as Table 8.

Figure 19 shows results changes in the cavity diameter with cavity length between 10 and 50 mm. It confirmed extension of cavity diameter due to simulated repetitive operation of 10,000 shots in all cavity length. In short cavity length case, it considered to extend cavity diameter due to repetitive operation because it increased ablation per unit area by raised energy density. In long cavity length case, it considered to restrain extension of cavity diameter due to repetitive operation because it increased ablation per unit area by raised energy density. Therefore, it confirmed to affect extension of cavity diameter changing in the energy density by cavity length with repetitive operation.

In results of this simulation, it confirmed high impulse bit and longtime operation, considered optimum with cavity length at 50 mm for orbital transfer by 50 kg class nano-satellite. Simulation in cavity length at 50 mm carried out repetitive operation of 50,000 shots. Figure 20 shows impulse bit and cavity diameter versus shot number. In results, the simulation decreased impulse bit of 0.96 mNs in repetitive operation of 50,000 shots, confirmed to extend cavity diameter to 13.8 mm, achieved a total impulse of 67.1 Ns.

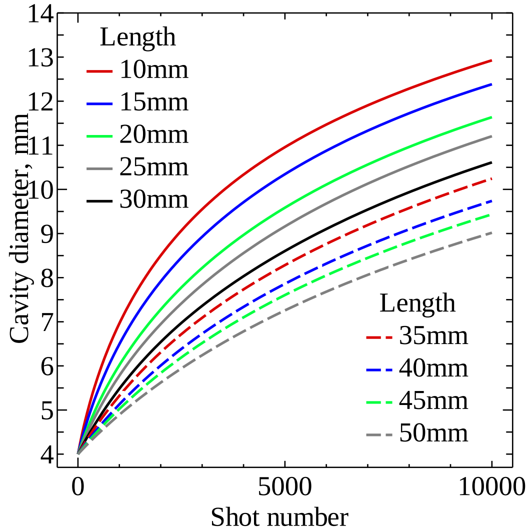

Figure 19. Changes in the cavity diameter as every cavity length.

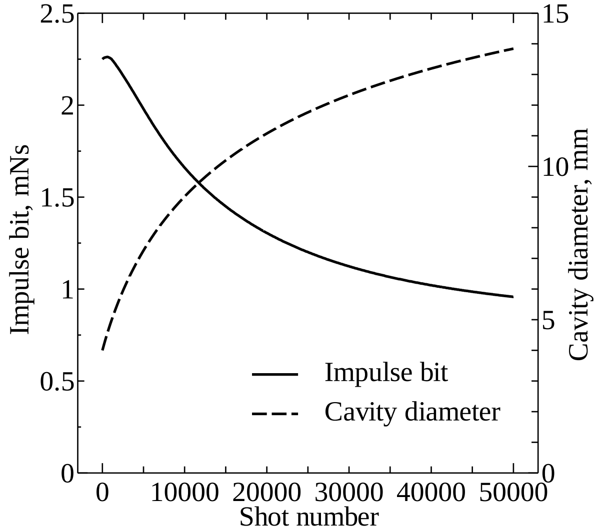

Figure 20. Impulse bit and cavity diameter vs. shot number.

B. Experiment

In order to achieve longer lifetimes a MDR-PPT was developed. The MDR-PPT has many discharge rooms with each one ignitor. The ignitors are operated by the PPU. The final thruster is shown in Fig. 21 and the specifications are shown in Table 9. Now the MDR-PPT consists of seven single-PPTs (S-PPTs) and thus a uniform mounting of the single thrusters could be achieved. The S-PPT was used to do a repetitive operation experiment.

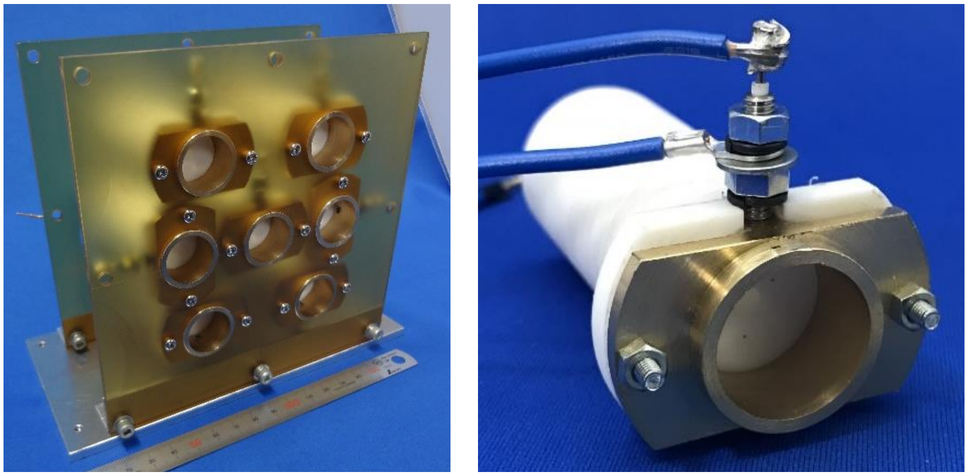

Figure 21. MDR-PPT and S-PPT.

Table 9. Specification of MDR-PPT.

Size, mm	90 x 226 x 155
Mass, kg	1.33
Number of discharge room	7
Discharge room diameter, mm	4
Discharge room length, mm	50
Cathode diameter, mm	20
Cathode length, mm	14
Input energy, J	31.59
Operational frequency, Hz	0.67

The S-PPT was able to accomplish round about 114,000 shots with a total impulse of 100 Ns. The impulse bit results during the experiment are presented in Fig. 22. The generated total impulse would be sufficient to propel a 50 kg nano-satellite for approximately 25 km.

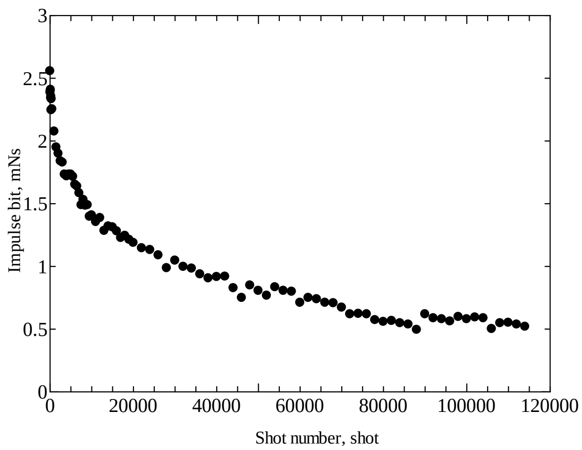

Figure 22. Impulse bit vs. shot number.

Finally, a mass of 2.47 kg for the capacitors, 0.5 kg for the circuit board 1.33kg for the MDR-PPT could be achieved. Thus, the mass of the entire MDR-PPT system is approximately 5.3 kg. The assembled MDR-PPT system is shown in Fig. 23.

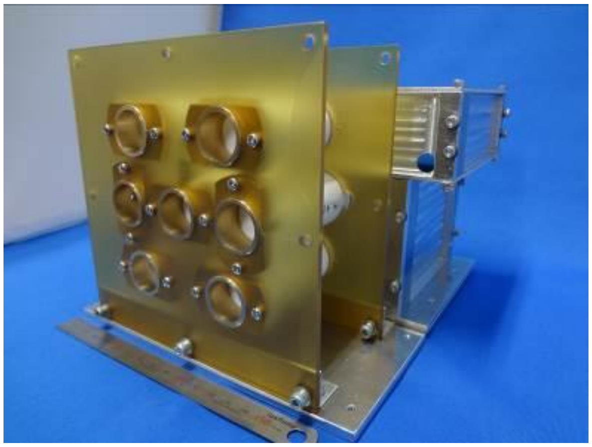

Figure 23. MDR-PPT system.

C. Conclusion

The Project of Osaka Institute of Technology Electric-Rocket-Engine onboard Small Space Ship (PROITERES) was started at Osaka Institute of Technology in 2007. Now, we are developing the 2nd PROITERES satellite. The R&D of the 2nd PROITERES was started in 2010. The main mission is to achieve longer distance orbital transfer, i.e. changing 50-100 km in altitude on near-earth orbits by longtime operation and high power PPT system. It has been decided that the 50kg class 2nd PROITERES satellite is launched to 613 km in earth altitude by H-IIA rocket at Tanegashima Space Center, Japan Aerospace Exploration Agency (JAXA) on July in 2008. The 2nd PROITERES satellite will be launched by piggyback payloads of GOSAT-2 and Khalifasat. This research aims to develop 30 W class PPT system by numerical calculation and experiment. In numerical calculation, it confirmed high impulse bit and longtime operation, considered optimum with cavity length at 50 mm for orbital transfer by 50 kg class nano-satellite. In experiment, longer lifetimes a MDR-PPT was developed. The MDR-PPT consists of seven single-PPTs and thus a uniform mounting of the single thrusters could be achieved. The S-PPT was able to accomplish round about 114,000 shots with a total impulse of 100 Ns.

V.Hall thruster

Figure 24 shows the Anode-Layer-Type Hall thruster (TAL-type) and the Magnetic-Layer-Type Hall thruster (SPT-Type) and the Cylindrical-Type Hall thruster (CHT-type). The high-power TAL and SPT types are studied for manned Mars exploration, and the CHT-type will be equipped in nano-satellite for powered-flight to Moon.

Furthermore, in Japan, a project named "Robust Anode-layer Intelligent for Japan IN-space propulsion" (RAIJIN) was started in 2012. The RAIJIN project aims to develop Japanese high-power Hall thruster systems for future space missions. In this project the task of Osaka Institute of Technology (OIT) is the evaluation of the high voltage operation characteristics with RAIJIN94 thruster, as shown in Fig. 24 (c)[20-24].

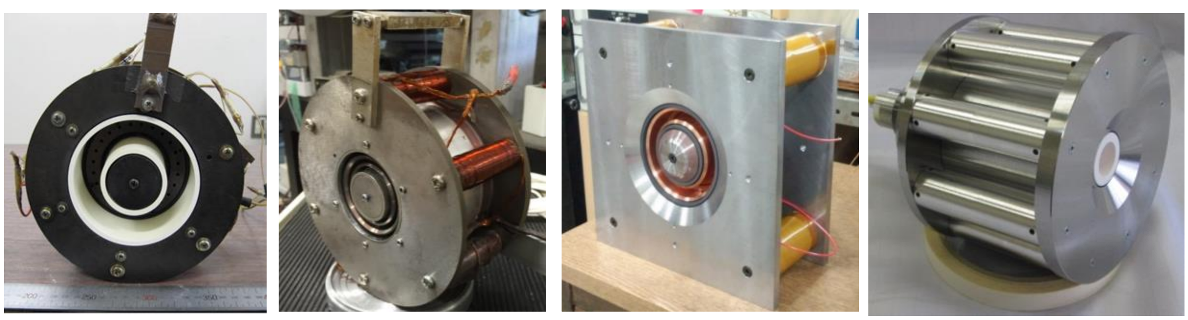

(a) SPT-type **(b) TAL type** **(c) RAIJIN94 of TAL type** **(d) CHT type**

Figure 24. Hall thruster at OIT.

A. SPT-type THT-VI

The experimental conditions of THT-VI are shown in Table 10. To confirm the stability of the operation the discharge voltage was increased in increments of 100 V from 300 V to 1,000 V. The experiments were carried out with two different propellant mass flow rates, which were 3.0 mg/s and 4.0 mg/s.

Table 10. Experimental condition of THT-VI.

Discharge Voltage	300-1,000 V	
Propellant	Xenon	
Mass Flow Rate	THT-VI	3.0, 4.0 mg/s
	Hollow Cathode	0.1 mg/s
Coil Current	0.45 A, 0.45 A, 0.6 A (Outer, Inner, Trim)	
Back Pressure	6.0 x 10^{-2} Pa	
Chamber Facility	OIT	

Figure 25 (a) shows the discharge current (A) - discharge voltage (V) graph, Figure 25 (b) shows the thrust (mN) - discharge voltage (V) graph, Figure 25 (c) shows specific Impulse (s) - discharge voltage (V) graph and Figure 25 (d) shows thrust efficiency (%) - discharge voltage (V) graph. In these experiments, both propellant mass flow rates were successfully tested up to discharge voltages of 1,000 V.

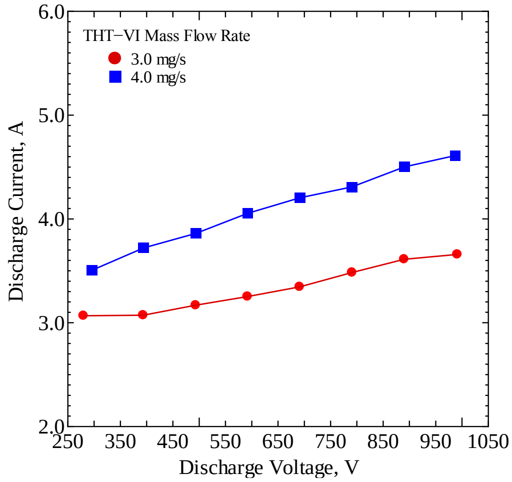

(a) Discharge current vs. discharge voltage

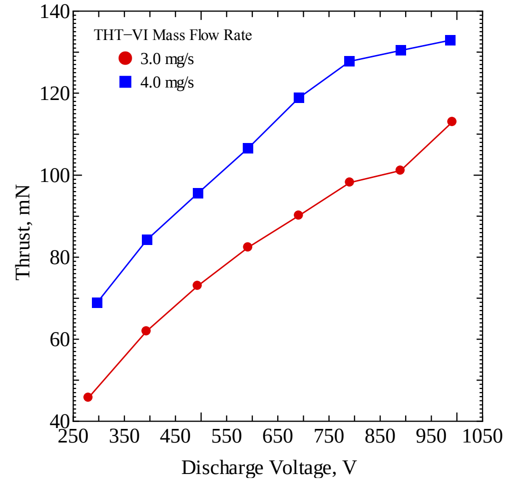

(b) Thrust vs. discharge voltage

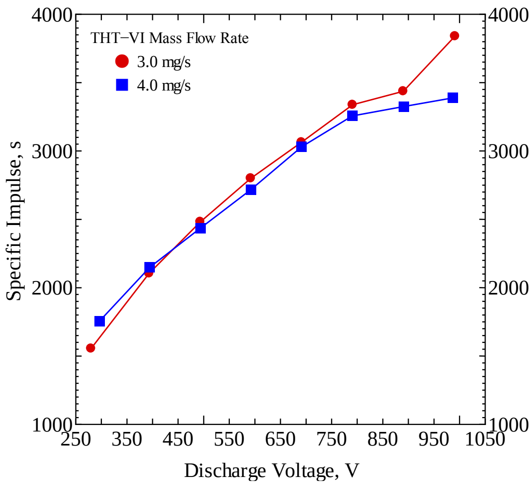

(c) Specific impulse vs. discharge voltage

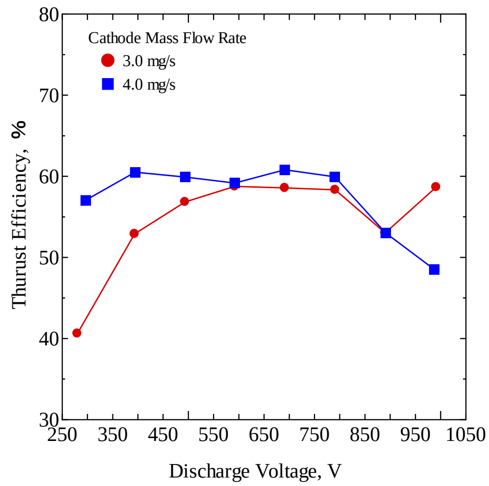

(d) Thrust efficiency vs. discharge voltage

Figure 25. Experimental results of THT-VI.

B. TAL type TALT-2B

In previous operation tests, it was found out that the operation in the high voltage region is difficult due to the burnout of the outer coil, the melting of the anode, and the breakage of the ceramics which are the result of the thermal expansion of the anode. Therefore, OIT developed a TALT-2B which improved the thruster head while preserving the shape of the discharge chamber. The first point of improvement is that the outer coil was changed from a one ring - shaped air core coil to six cored coils. The idea behind this change was that the burnout can be avoided by the separation of the outer coil from the discharge chamber. The second point is that gaps are formed in the ceramics around the anode. The damage of the ceramics was caused by the absence of gaps. In detail, a large gap was added by fitting the ceramics together.

The experimental conditions of TALT-2B are shown in Table 11. To confirm the stability of the operation the discharge voltage was increased successfully from 300 V to 500 V.

Table 11. Experimental conditions of TALT-2B.

Discharge Voltage	300-500 V	
Propellant	Xenon	
Mass Flow Rate	TALT-2B	3.0 mg/s
	Hollow Cathode	0.1 mg/s
Coil Current	1.2 A, 2.0 A, 2.0 A (Outer, Inner, Trim)	
Back Pressure	6.0 x 10^{-2} Pa	
Chamber Facility	OIT	

The experimental results like discharge voltage, discharge current, thrust, specific impulse and thrust efficiency are presented in Table 12.

In general, the discharge current was relatively high on the one side, and the thrust and the specific impulse was relatively low on the other side. Although this experiment was essentially planned to be performed up to 1,000 V, the experiment was stopped because it turned out that operation of the head and the anode became unstable at 600 V. After the experiment, we could find out that the anode melted in the red hot portion and burnout of the inner coil occurred.

Table 12. Experimental results of TALT-2B.

Discharge Voltage	300 V	400 V	500 V
Discharge Current	4.6 A	5.4 A	6.2 A
Thrust	37 mN	44 mN	50 mN
Specific Impulse	1260 s	1490 s	1690 s
Thrust Efficiency	16%	15%	13%

C. TAL type RAIJIN94

RAIJIN 94 was produced at the "Department of Advanced Energy Engineering Science, Graduate School of Engineering Sciences, Kyushu University", with the aim of developing a 10 kW class Anode-Layer type Hall thruster. The previous stage of the thruster was 5 kW.

The experimental conditions for “RAIJIN94” are shown in Table 13. We could confirm the operation in increments of 50 V from a discharge voltage of 300 V to 1,000 V. Experiments were carried out with two different propellant: Xenon, Krypton. This experiment was conducted with JAXA's experimental facility.

Table 13. Experimental conditions of RAIJIN94.

Discharge Voltage	300-1,000 V	
Propellant	Xenon, Krypton	
Mass Flow Rate	RAIJIN94	3.0 mg/s
	Hollow Cathode	0.1 mg/s
Coil Current	0.8 A, 0.8 A, 2.0 A (Outer, Inner, Trim)	
Back Pressure	3.0 x 10^{-2} Pa	
Chamber Facility	JAXA	

Figure 26 shows the discharge current (A) - discharge voltage (V) graph, the thrust (mN) - discharge voltage (V) graph, the specific Impulse (s) - discharge voltage (V) graph and thrust efficiency (%) - discharge voltage (V) graph.

During krypton operation, red heat was observed at the anode at a discharge voltage of 850 V. Thus, the experiment was stopped. Essentially, thrust, specific impulse and thrust efficiency should all increase proportional to the input voltage in case of Hall thrusters. But in the experiments only the thrust and specific impulse showed a linear increase, the thrust efficiency had a decreasing behavior.

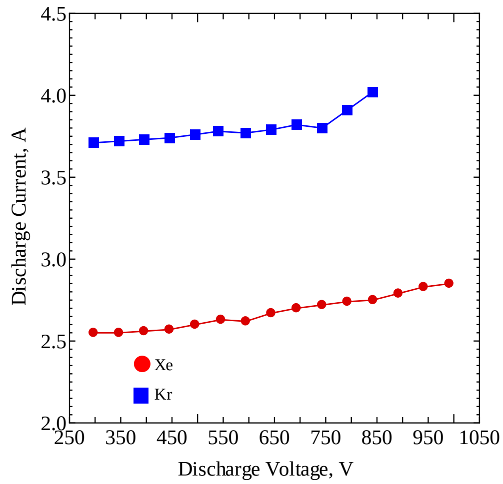

(a) Discharge current vs. discharge voltage

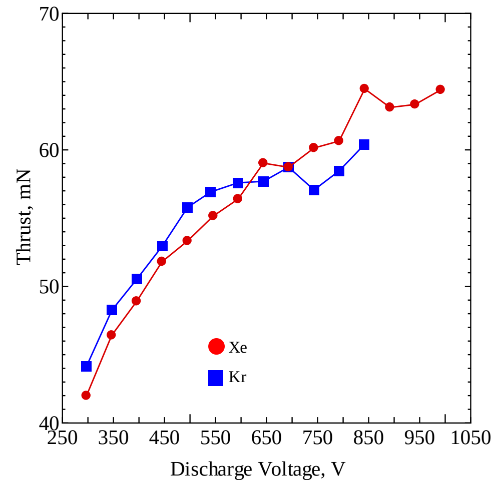

(b) Thrust vs. discharge voltage

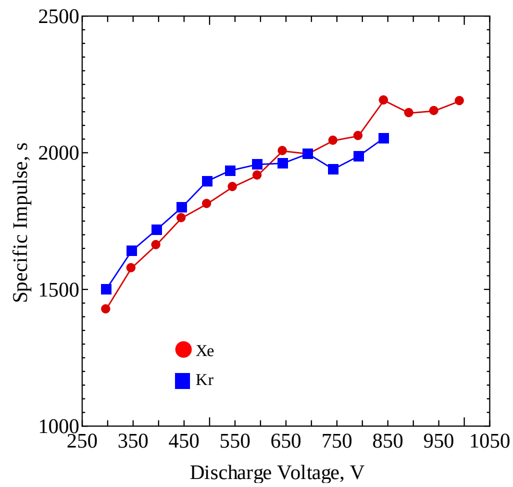

(c) Specific impulse vs. discharge voltage

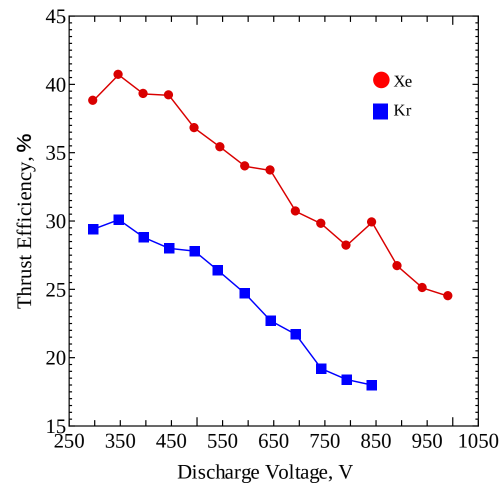

(d) Thrust efficiency vs. discharge voltage

Figure 26. Experimental results of RAIJIN94

D. CHT type TCHT-5

The TCHT-5 is a cylindrical-type hall thruster. The discharge channel made of Boron Nitride (BN) and the inner diameter is 14 mm. Xenon is used as the propellant. Furthermore, TCHT-5 can be changed the anode position and the discharge room length by a screw mechanism. The anode position can be moved by changing magnetic pole position.

Table 14 shows the experimental condition A of the TCHT-5. Discharge voltage was changed every 50 V in 150-1,000 V, and mass flow rate was changed every 0.05 mg/s in 0.3-0.4 mg/s. However, the TCHT-5 was not operating at the discharge voltage above 950 V with Xm = 22 mm, Xd = 12 mm, and the mass flow rate of 0.35 mg/s. Similarly, the TCHT-5 was not operating at the discharge voltage above 850 V with the mass flow rate of 0.4 mg/s.

Table 14. Experimental conditions of TCHT-5.

Discharge voltage	150 – 1,000 V	
Propellant	Xenon	
Mass flow rate	TCHT-5	0.3-0.4 mg/s
	Hollow cathode	0.1 mg/s
Back pressure	4.0×10^{-2} Pa	

The experimental results when mass flow rate was 0.3mg/s of TCHT-5 is shown below. Figure 27 show the specific impulse (s) – input power (W) graph and the thrust efficiency (%) – input power (W) graph.

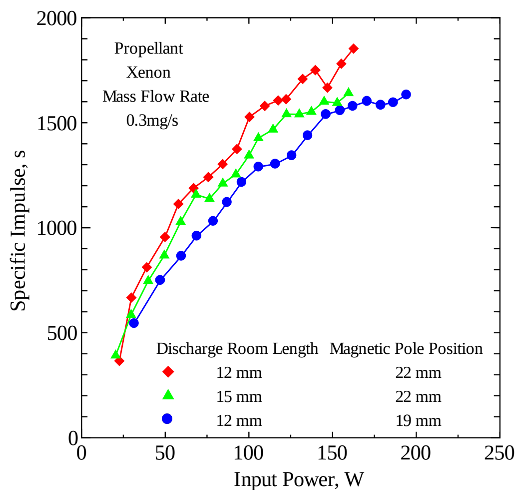

(a) Specific Impulse vs. input power

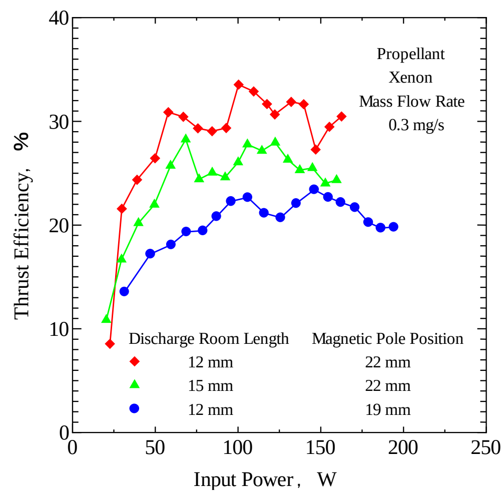

(b) Thrust efficiency vs. input power

Figure 27. Experimental results of TCHT-5.

E. Conclusion

Three types of Hall thruster have been investigated at OIT. The high-power TAL and SPT types are studied for manned Mars exploration, and the CHT-type will be equipped in the 3rd PROITERES nano-satellite for powered-flight to Moon. In order to achieve all missions, we are designing special structures of Hall thruster system with long lifetime. Furthermore, in Japan, a project named "Robust Anode-layer Intelligent for Japan IN-space propulsion" (RAIJIN) was started in 2012. In this project the task of Osaka Institute of Technology (OIT) is the evaluation of the high voltage operation characteristics with RAIJIN94 thruster. We have carry out performance evaluation of these Hall thrusters by experiment.

VI. Concluding Remarks

At Osaka Institute of Technology, four kinds of electric propulsions have been investigated and developed. Therefore, We have carry out performance evaluation and prediction of these electric propulsions by experiment and analysis.

References

[1]Saito, S., Chino, K., Sugiyama, Y., Tahara, H. and Takada, K., "Performance Characteristics of High-Power Steady-State MPD Thrusters with Cusp Field Using Permanent Magnets for Manned Mars Exploration", 31st International Symposium on Space Technology and Science, Paper No. ISTS 2017-b-25, Himegin Hall, Matsuyama-Ehime, Japan, 2017.

[2]Chino, K., Saito, S., Sugiyama, Y., Tahara, H. and Takada, K., "Thermal Analysis of Steady-State Fully Radiation-Cooled MPD Thrusters using Permanent Magnets for Manned Mars Exploration", 31st International Symposium on Space Technology and Science, Paper No. ISTS 2017-b-65p, Himegin Hall, Matsuyama-Ehime, Japan, 2017.

[3]Sugiyama, Y., Chino, K., Saito, S., Hirokazu, T. and Kyoko, T., "Research and Development of High-Power Steady-State MPD Thrusters with Permanent Magnets and Hollow Cathodes for In-Space Propulsion", Space Propulsion 2016, Paper No. 3124902, Marriott Rome Park Hotel, Roma, Italy, 2016.

[4]Suzuki, T., Koyama, N., Sugiyama, Y., Sakoda, H. and Tahara, H., "Performance Characteristics of Steady-State MPD Thrusters with Permanent Magnets and Multi Hollow Cathodes for Manned Mars Exploration", Joint Conf.: 30th International Symposium on Space Technology and Science (30th ISTS), 34th International Electric Propulsion Conference (34th IEPC), 6th Nano-Satellite Symposium (6th NSAT), IEPC-2015-197/ ISTS-2015-b-197, Kobe, Japan, 2015.

[5]Sugiyama, Y., Koyama, N., Suzuki, T., Sakoda, H. and Tahara, H., "Thermal Characteristics of Radiation-Cooled Steady-State MPD Thrusters with Permanent Magnets and Multi Hollow Cathodes for In-Space Propulsion", Joint Conf.: 30th International Symposium on Space Technology and Science (30th ISTS), 34th International Electric Propulsion Conference (34th IEPC), 6th Nano-Satellite Symposium (6th NSAT), IEPC-2015-198/ ISTS-2015-b-198, Kobe, Japan, 2015.

[6]Fukutome, Y., Shiraki, S., Matsumoto, K., Inoue, F., Tahara, H., Nogawa, Y. and Momozawa, A., "Performance Characteristics of Low-Performance Arcjet Thrusters using Low –Toxicity Propellants of HAN", Joint Conf.: 30th International Symposium on Space Technology and Science (30th ISTS), 34th International Electric Propulsion Conference (34th IEPC), 6th Nano-Satellite Symposium (6th NSAT), IEPC-2015-229/ISTS-2015-b-229, Kobe, Japan, 2015.

[7]Shiraki, S., Fukutome, Y., Inoue, F., Matsumoto, K., Tahara, H., Nogawa, Y. and Momozawa, A., "Performance Characteristics of Low-Power Arcjet Thruster Systems with Gas Generators for Water", Joint Conf.: 30th International Symposium on Space Technology and Science (30th ISTS), 34th International Electric Propulsion Conference (34th IEPC), 6th Nano-Satellite Symposium (6th NSAT), IEPC-2015-230/ISTS-2015-b-230, Kobe, Japan, 2015.

[8]Inoue, F., Fukutome, Y., Shiraki S., Matsumoto, K. and Tahara, H., "Performance and Thermal Characteristics of High-Power Hydrogen Arcjet Thrusters with Radiation-Cooled Anodes for In-Space Propulsion", Joint Conf.: 30th International Symposium on Space Technology and Science (30th ISTS), 34th International Electric Propulsion Conference (34th IEPC), 6th Nano-Satellite Symposium (6th NSAT), IEPC-2015-231/ISTS-2015-b-231, Kobe, Japan, 2015.

[9]Fukutome, Y., Shiraki, S., Inoue, F., Shimogaito, K., Nakanishi, T., Tahara, H., Takada, K., Nogawa, Y. and Momozawa, A., "Research and Development of High-Power Steady-State MPD Thrusters with Permanent Magnets and Hollow Cathodes for In-Space Propulsion", Space Propulsion 2016, Paper No. 3124902, Marriott Rome Park Hotel, Roma, Italy, 2016.

[10]Shiraki, S., Tahara, H., "Performance and Thermal Characteristics of Low-Power DC Arcjet Thrusters with Radiation-Cooled Anodes for Green Propellants", AIAA Propulsion and Energy Forum and Exposition (Propulsion and Energy 2016), AIAA-2016-4700, Salt Lake City, USA, 2016.

[11]Mimura, T., Fukutome, Y., Shiraki, S., Shimogaito, K., Okuda, K., Tahara, H., Takada, K., Momozawa, A., Nogawa, Y. and Nakata, D., "Performance Characteristics of Low-Power DC Arcjet Thrusters with Low-Toxicity Propellants", 31st International Symposium on Space Technology and Science, Paper No. ISTS 2017-a-38, Himegin Hall, Matsuyama-Ehime, Japan, 2017.

[12]Okuda, K., Fukutome, Y., Shiraki, S., Shimogaito, K., Mimura, T., Tahara, H., Takada, K., Momozawa, A., Nakata, D. and Nogawa, Y., "Research and Development of Low-power Anode-Radiation-Cooled DC Arcjet Thruster Using Water Propellants", 31st International Symposium on Space Technology and Science, Paper No. ISTS 2017-b-42, Himegin Hall, Matsuyama-Ehime, Japan, 2017.

[13]Kamimura, T., Nishimura, Y., Ikeda, T. and Tahara, H., "R&D and Final Operation of Osaka Institute of Technology 1st PROITERES Nano-Satellite with Electrothermal Pulsed Plasma Thrusters and Development of 2nd and 3rd Satellites", Joint Conf.: 30th International Symposium on Space Technology and Science (30th ISTS), 34th International Electric Propulsion Conference (34th IEPC), 6th Nano- Satellite Symposium (6th NSAT), IEPC-2015-209/ISTS-2015-b-209, Kobe, Japan, 2015.

[14]Fujita, R., Fujita, H., Yamauchi, T., Kajihara, K., Yagi, R., Tahara, H., Takada, K. and Ikeda, T., "Research and Development of Osaka Institute of Technology PROITERES Series Nano-Satellites with Electric Propulsion", 31st International Symposium on Space Technology and Science, Paper No. ISTS 2017-b-66p, Himegin Hall, Matsuyama-Ehime, Japan, 2017.

[15]Fujita, R., Muraoka, R., Kanaoka, K., Huanjun, C., Tanaka, M., Tahara, H. and Wakizono, T., "Flowfield Simulation and Performance Prediction of Electrothermal Pulsed Plasma Thrusters Onboard Osaka Institute of Technology PROITERES Nano-Satellite Series", Joint Conf.: 30th International Symposium on Space Technology and Science (30th ISTS), 34th International Electric Propulsion Conference (34th IEPC), 6th Nano- Satellite Symposium (6th NSAT), IEPC-2015-207/ISTS-2015-b-207, Kobe, Japan, 2015.

[16]Fujita, R., Haase, T., Kanaoka, K., Ono, K., Morikawa, N., Ryuho, K., Enomoto, K., Tahara, H., Takada, K. and Wakizono, T., "One-Dimensional Flowfield Calculation of Coaxial Pulsed Plasma Thrusters", 31st International Symposium on Space Technology and Science, Paper No. ISTS 2017-b-48, Himegin Hall, Matsuyama-Ehime, Japan, 2017.

[17]Fujita, R., Muraoka, R., Ikeda, T., Kanaoka, K., Tahara, H. and Wakizono, T., "Development of Electrothermal Pulsed Plasma Thruster Systems for Powered Flight of Micro-Satellites", Frontier of Applied Plasma Technology, Vol.8, No.1, pp.19-24, 2015.

[18]Kanaoka, K., Fujita, R., Muraoka, R., Tahara, H. and Wakizono, T., "Research and Development of High-Power Electrothermal Pulsed Plasma Thruster Systems for Osaka Institute of Technology 2nd PROITERES Nano-Satellite", Joint Conf.: 30th International Symposium on Space Technology and Science (30th ISTS), 34th International Electric Propulsion Conference (34th IEPC), 6th Nano-Satellite Symposium (6th NSAT), IEPC-2015-22/ISTS-2015-b-22, Kobe, Japan, 2015.

[19]Kanaoka, K. and Tahara, H., "Research and Development of a High-Power Electrothermal Pulsed Plasma Thruster System onboard Osaka Institute of Technology 2nd PROITERES Nano-Satellite", AIAA Propulsion and Energy Forum and Exposition, AIAA-2016-4844, Salt Lake City, Utah, USA, 2016.

[20]Takahata, Y., Kakuma, T., Kagota, T., Nishida, M., Ikeda, T. and Tahara, H., "Research and Development of High-Power, High-Specific-Impulse Magnetic-Layer-Type Hall Thrusters for Manned Mars Exploration", Joint Conf.: 30th International

Symposium on Space Technology and Science (30th ISTS), 34th International Electric Propulsion Conference (34th IEPC), 6th Nano-Satellite Symposium (6th NSAT), IEPC-2015-151/ISTS-2015-b-151, Kobe, Japan, 2015.

[21]Kagota, T., Takahata, Y., Kakuma, T., Nishida, M., Ikeda, T. and Tahara, H., "Performance Characteristics of High-Power, High-Specific-Impulse Anode-Layer-Type Hall Thrusters for In-Space Propulsion" Joint Conf.: 30th International Symposium on Space Technology and Science (30th ISTS), 34th International Electric Propulsion Conference (34th IEPC), 6th Nano-Satellite Symposium (6th NSAT), IEPC-2015-153/ISTS-2015-b-153, Kobe, Japan, 2015.

[22]Kakuma, T., Ikeda, T., Nishida, M., Kagota, T., Takahata, Y., Tahara, H., "Research and Development of Low-Power Cylindrical-Type Hall Thrusters for Nano/Micro-Satellites", Joint Conf. 30th International Symposium on Space Technology and Science (30th ISTS), 34th International Electric Propulsion Conference (34th IEPC), 6th Nano-Satellite Symposium (6th NSAT), IEPC-2015-302/ISTS-2015-b-302, Kobe, Japan, 2015.

[23]Takahata, Y., Kagota, T., Kakuma, T., Kobayashi, M., Furukubo, Y., Tahara, H., Takada, K. and Ikeda, T., "Hall Thruster R&D Activities at Osaka Institute of Technology", Space Propulsion 2016, Paper No. 3124904, Marriott Rome Park Hotel, Roma, Italy, 2016.

[24]Kakuma, T. and Tahara, H., "Research and Development of low-Power and High-Power Three-Types Hall Thrusters at Osaka Institute of Technology", AIAA Propulsion and Energy Forum and Exposition (Propulsion and Energy 2016), AIAA-2016-4944, Salt Palace Convention Center, Salt Lake City, Utah, USA, 2016.